Preprints (www.preprints.org) | NOT PEER-REVIEWED | Posted: 4 June 2020

Peer-reviewed version available at *Appl. Sci.* **2020**, *10*, 4498; doi:10.3390/app10134498

Article

NSHT: New Smart Hybrid Transducer for Structural and Geotechnical Applications

Vincenzo Minutolo[1]*(V.M.), Enis Cerri[1](E.C.), Agnese Coscetta[1](A.C.), Emilia Damiano[1](E.D.), Martina De Cristofaro[1](M.D.), Luciana Di Gennaro[1](L.D.), Luca Esposito[1](LE), Paolo Ferla[1](P.F.), Maurizio Mirabile[2](M.M.). Lucio Olivares[1](L.O.) and Renato Zona[1](R.Z.)

[1] Department of Engineering Università degli Studi della Campania "Luigi Vanvitelli" Via Roma 29 - 81031 Aversa (CE), Italy.-mail: dip.ingegneria@unicampania.it - Web page: https://www.unicampania.it

[2] HPSYSTEM srl, Via Papini n.12 – San Giorgio a Cremano (NA), Italy, e-mail:info@hpsystem.it – Web page: https://hpsystem.it

* Correspondence: vincenzo.minutolo@unicampania.it; Tel.: +39-081-5010-305

Featured Application: The proposed work provided a structural transducer able to measure continuously in time and space the strain on linear structures. The transducer has been realized connecting fiber-reinforced tapes and optical fiber sensors. It has been possible, then, to overcome some weaknesses of traditional optical fiber sensors like fragility and critical positioning in actual civil structures. The system has been tested in some real scale examples and is seen that satisfy the requirements of easy on-site applications. The feasibility of the sensor and the transducer allow using it in connection with fiber-reinforced tapes as an integrated system for smart structural reinforcement as well that can be used for continuous health monitoring of structures consequent to restoration and repair.

Abstract: This work describes the application of a new transducer prototype for continuous monitoring both in the structural and geotechnical fields. The transducer is synthetically constituted by a wire of optical fiber embedded between two fiber tapes (fiberglass or carbon fiber) and glued by a matrix of polyester resin. The fiber optical wire ends have been connected to a control unit whose detection system is based on Brillouin optical time-domain frequency analysis. Three laboratory tests were carried out to evaluate the sensor's reliability and accuracy. In each experiment, the transducer was applied to a sample of inclinometer casing sets in different configurations and with different constraint conditions. The experimental data collected were compared with theoretical models and with data obtained from the use of different measuring instruments to perform validation and calibration of the transducer at the same time. Several diagrams allow comparing the transducer and highlighting its suitability for monitoring and maintenance of structures. The characteristic of the transducer suggests its use as a mixed system for reinforcing and monitoring, especially in lifetime maintenance of critical infrastructures such as transportation and service networks, and historical heritage.

Keywords: Structural safety assessment; experimental monitoring; strain transducers; reinforcement; civil engineering; optical fiber sensors; lifetime structural monitoring; Brillouin.

1. Introduction

An increasing number of territories and engineering works are seriously threatened by a combination of adverse effects related to natural disasters (e.g., landslides, earthquakes) or human-made causes (such as traffic-induced vibrations, degradation of structures, absence of maintenance). This problem mainly affects the countries characterized by old infrastructures and old towns of historical, artistic, and cultural interests.

© 2020 by the author(s). Distributed under a Creative Commons CC BY license.

Preprints (www.preprints.org) | NOT PEER-REVIEWED | Posted: 4 June 2020

Peer-reviewed version available at Appl. Sci. 2020, 10, 4498; doi:10.3390/app10134498

In this context, it becomes essential to develop Early Warning Systems (EWS) to quickly detect potentially dangerous events occurred in specific areas or on engineering works [1] to define an appropriate intervention strategy consisting of stabilization works or structural reinforcements.

Several studies [2, 3, 4] and analyses exist in the literature that used conventional transducers, among the others, for structural and geotechnical EWS or SHM (Structural Health Monitoring).

Generally, such procedures used local sensors as strain gauges, accelerometers, laser sensors, doppler, and reticles with multicore optical fiber.

Damaged buildings, monuments, cavities, and infrastructures are significantly increasing due to the broader exposed areas to natural hazards and due to the old age of the civil constructions and require a strong effort for their surveillance and maintenance. In this context, it becomes essential to develop innovative Early-Warning Systems (EWS), as well as Structural Health Monitoring and Reinforcement (SHMR), able to detect any anomalous behavior [5, 6, 7, 8]. These systems contain conventional and unconventional, distributed, and local sensors. These EWSs allows collecting the information and managing them remotely.

In the following report, two experimental approaches have been described. One concerns the development of a New Hybrid Distributed Transducer to be used both for the detection of landslide movements and for structural monitoring and reinforcement. The second approach consists of the development of a smart system of local sensors based on a wired data acquisition system to collect and analyze structural data from different locations in a structure. The measured data is addressed toward a central acquisition unit that can be interrogated remotely. The approach exploits the variety of low-cost sensors included in a smartphone and a set of libraries protocols and programming tools (API).

Regarding the first approach, in the laboratories of Department of Engineering of the University of Campania, "Luigi Vanvitelli" distributed strain and temperature measurement devices have been developed using an optical fiber cable for communications as a sensor. The proposed method is based on a technique described in [9]. The acquisition system is based on the device reported in [10]. The system allows measuring temperature and strain as high as 10 $\mu\varepsilon$ along with the fiber with a spatial resolution of about $0.8m$ at a low frequency ($0.1Hz$).

Such type of distributed strain measurements can be performed in slopes or along with linear infrastructures even over long distances representing a significant advantage for conventional pointwise strain measurements (topographic measurements, inclinometers, strain gauges, among the others), which can provide only local data, with the risk of missing critical points, [11].

Several applications of optical fiber as strain sensors in the geotechnical field have been performed in the past years. Iten and Puzrin [12] used optical fiber embedded in a natural slope subjected to extremely slow movement to locate the boundaries of the sliding mass. Examples of seepage and strain monitoring systems realized by using optical fiber sensors in embankment dams can be found in [13, 14], and other applications are available in geosynthetics and reinforced soil slopes used on artificial and small-scale physical models [15, 16].

Optical fibers have also been used for the measurement of soil displacement profiles based on the principle of the inclinometer tube [17, 18]. The work presented in [19], describes one of the first applications in an embankment slope, *ad hoc* instrumented with inclinometers with optical fiber sensors glued on. The described set up shows the suitability of that array of sensors to detect soil strain increasing during rainwater infiltration. However, the cost of such type of monitoring was not competitive, and also technical problems due to the instrumentation of the inclinometer's tubes made this application only a prototype. Moreover, most of these researches were based on Fiber Bragg Grating (FBG) sensing technique [20, 21, 22, 23]: with this method, only small portions of the optical cable constitute the sensors. The FBG sensors connected and glued onto the surface of a plastic rod for measuring bending strains and axial strains give pointwise information along the inclinometer tube. In landslide detection, where often the sliding surface localizes in a very narrow shear band, pointwise measurements can fail to recognize actual soil movements. Consequently, distributed sensing results in a more effective tool

Preprints (www.preprints.org) | NOT PEER-REVIEWED | Posted: 4 June 2020

Peer-reviewed version available at Appl. Sci. 2020, 10, 4498; doi:10.3390/app10134498

In [24,25, 26], further investigation on landslide monitoring using physical models highlights the difficulties in setting up and analyze the coupling between the soil and the sensor. Moreover, since the optical fiber sensor is simply embedded into the soil, it is recognized that the strain transfer between the soil and the sensor is not wholly ensured, and it also depends on the overburden pressure.

Qualification and surveillance of structures require testing and monitoring that usually are made using pointwise sensors. The acquisition time is limited to the initial lifetime of the structure or at the end of manufacturing. Several analyses for SHMR can be found in literature based on ultrasonic testing [27, 28], thermography [29, 30], and measurements of static deformation and dynamic vibrations [31, 32]. Moreover, some static stress and dynamic vibration analysis using strain gauges, accelerometers [33] or contactless laser

Doppler vibrometers, broadband reflection gratings with multicore optical fiber [34, 35, 36] are often described. However, many research works emerge that one of the best challenges of SHMR is to prevent the sensor from damage [37, 38, 39]. In this respect, optical fibers for telecommunications, which are the sensing devices when BODTA is used, are very robust and do not suffer time or chemical degradation, provided the fiber be adequately protected from mechanical injuries as it is the case of the sensor here proposed [40, 41].

Barrias and Bao describe the evolution of the SHMR with a review of the major experiments and results carried out to date and show the effectiveness of the use of optical fiber sensors [42, 43].

Many works describe embedded sensors for different types of structures: reinforced concrete wall, pre-stressed concrete bridge [44], the optical fiber in wind turbine blade [45], integrated optical fiber in functionalized carbon structures (FCS) [46] and also for the detection of vibration, surface cracking and buckling phenomena [47, 48, 49] in reinforced concrete, pre-stressed concrete (PSC) [50], and post-tensioned PSC [51] where the effectiveness of distributed sensors is highlighted.

In [46], it is reported an example of the integration of functionalized carbon structure with optical fiber sensing, but experimental results concerning integrated reinforcement and sensors are not yet present at actual authors' knowledge.

The present paper aims to show a prototype of an improved transducer (NSTH, New Smart Hybrid Transducer) that allows overcoming the drawbacks of traditional solutions based on pointwise sensors [52].

At first, one must specify that NSTH is a transducer that is a complex system of which the sensor is only one of the constituents.

The system allows continuous monitoring of engineering works and terrestrial portions, even for lengths of hundreds of meters, while providing information about mechanical deformations and thermal variations.

NHST can be assembled in implants and safely transported thanks to its design features that also allow avoiding breaking during transportation and installation, overcoming the drawbacks of existing solutions based on distributed sensors. [53, 54, 55, 56]

In this paper, we propose two examples of the application of NHST: the first as a smart inclinometer and the second as a Structural Health Monitoring and Reinforcement device (SHMR). In these two applications, we analyze the accuracy and the reliability of the NHST transducer using a conventional optical acquisition system.

In this work, the experimental analysis is presented describing the application of NSHT made of a BOTDA optical fiber sensor joined to mechanical support suited *ad hoc* designed to fulfill safety and secure handling during installation and lifetime. The proposed experiments allow considering the effectiveness of the system. Moreover, the correlation between hard measures and mechanical interpretation of structural behavior is proposed as well. The central aspect here considered is focused on the following point solution.

- the connection systems between the sensor and the element under observation do not realize a fully coupled stress transfer making the strain measurements only qualitative;
- the use of glue to fix the fiber on the structural element does not assure the possibility to perform long-time observation as it is unstable from a thermomechanical point of view and

Preprints (www.preprints.org) | NOT PEER-REVIEWED | Posted: 4 June 2020

Peer-reviewed version available at Appl. Sci. 2020, 10, 4498; doi:10.3390/app10134498

disconnections of the fiber in many points along the element can occur which vanish the efficiency of the system;
- when the sensor must be used in hard environments, such as slopes and rail tracks, where repeated long-time measurements must be done, it is necessary to realize appropriate coating of the fiber to avoid its damage;
- monitoring over long distances (in the order of several tens of meters) requires appropriate technical solutions for transporting and assembling the distributed transducer.

In subsequent sections, laboratory tests, results, and discussion on the application NSHT to simple beam structure and inclinometer tube have been reported.

2. Materials and Methods

Three different types of tests were carried out to validate the accuracy and reliability of the transducer measurements. The transducer is synthetically constituted by a wire of optical fiber embedded between two fiber tapes and glued by a matrix of polyester resin. Two kinds of sensors were made, the first merging two glass fiber tapes (GG) and the second pairing the glass tape with a carbon one (CG)

The fiber filament runs along with the support with a U-shaped path to determine an Inner segment and an Outer one, whose endpoints were connected to the control unit. There are fastening elements every 50 cm, to ensure perfect adhesion to the substrate. The configurations of the sensors are shown in the pictures below.

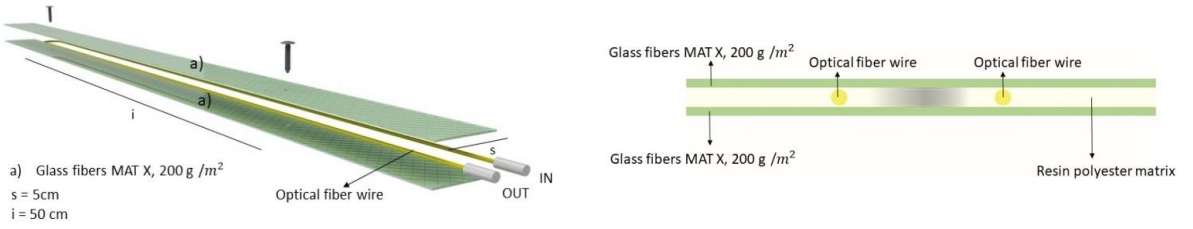

a) b)

Fig. 1 GG Transducer a) axonometric view, b) cross-section

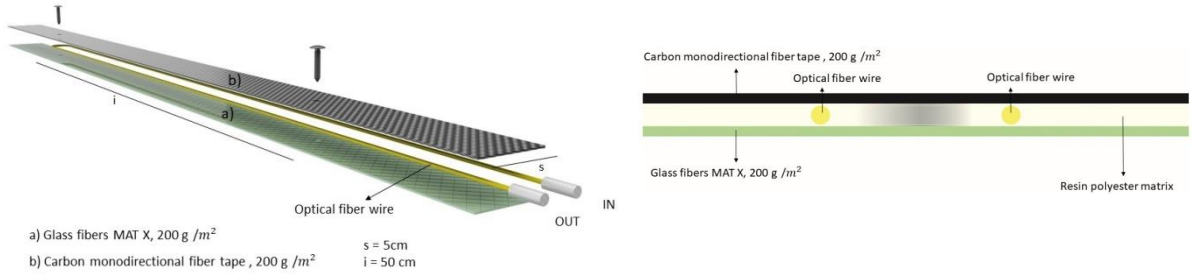

a) b)

Fig. 2 CG Transducer a) axonometric view, b) cross-section

Fig. 3 Transducer top view

This system was applied to the specimen constituted in an inclinometer casing, by a structural glue to ensure the perfect splinting of the elements.

Preprints (www.preprints.org) | NOT PEER-REVIEWED | Posted: 4 June 2020

Peer-reviewed version available at Appl. Sci. 2020, 10, 4498; doi:10.3390/app10134498

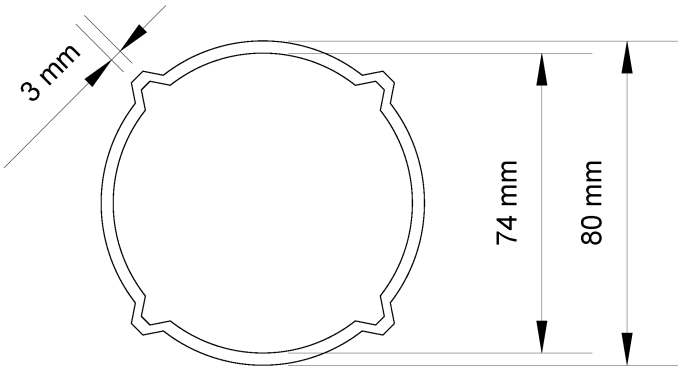

Fig. 4 Cross-section of inclinometer casing

The data acquisition is performed by control units with different levels of accuracy, whose detection system is based on Brillouin optical time-domain frequency analysis (BOTDA).

In the following paragraphs, both the materials used than the methods of data acquisition are described.

2.1 *First Test: Supported beam equipped with GG*

The tests aimed to evaluate the accuracy of the transducer by comparing experimental strain measures with the analytical results from beam theory.

The transducer was installed over a specimen that consists of an inclinometer casing (Fig 4). The structural scheme and the mechanical and geometrical properties are reported in figure (5) and table (1).

Tab. 1. First test - Geometrical parameters

Length [mm]	Radius [mm]	Thickness [mm]	Inertia [cm⁴]
7600	80	3	56.4871

The pipe was equipped with two sensors located at 90 degrees. The experimental setup is described in table 2:

Tab. 2. First test - Specimen parameters

Type	Structural glue	Fiber	Length [mm]	Optical fiber	Resin	Control unit	Resolution [mm]
GG	ADEKIT 140 by Axon (bi-component epoxy resin)	Glass – Glass	7400	G.657 single-mode optical fibers	POLIPLAST M608 M11 R	OPTO SENSING	400

During the experiment, the structure was subjected to increasing constrained displacement in the middle span section. The transducer has recorded the strain along with the structure at the following load step:

- $v = 0$
- $v = 2.5\ cm$
- $v = 4.5\ cm$
- $v = 6.5\ cm$

Preprints (www.preprints.org) | NOT PEER-REVIEWED | Posted: 4 June 2020

Peer-reviewed version available at Appl. Sci. 2020, 10, 4498; doi:10.3390/app10134498

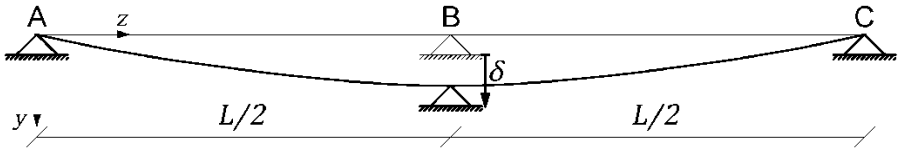

Fig. 5 First test – structural scheme

2.2 Experimental interpretation through flexure beam theory

In this section, the analytical solution of the bending beam is briefly recalled, and it is used for relating the measured strain with the expected deflection of the structure. The theoretical model of the beam is its axis, i.e., the straight line of the centroids of the cross-sections. The z axis of the reference frame coincides with the beam axis. The beam deforms into a line belonging to the vertical yz plane. The y coordinate of the curved line is the bending displacement $v(z)$.

Starting from the measured strains ε and knowing the aluminum tube radius, R, it was possible to calculate the beam curvature χ:

$$\chi = \frac{d\varphi}{ds} = \frac{d\varphi}{dz}\frac{dz}{ds} = -\frac{d\varphi'}{dz} = \frac{d^2v}{dz^2} \tag{1}$$

Recalling that under the Bernoulli's hypothesis of plane sections that remain perpendicular to the beam's deformed axis and the assumption that the displacements are infinitesimal, one obtains the curvature-displacement law:

$$\chi = \frac{d\varphi}{ds} = \frac{d\varphi}{dz}\frac{dz}{ds} = -\frac{d\varphi'}{dz} = \frac{d^2v}{dz^2} \tag{2}$$

By a first numerical integration of the χ function, one gets the rotation function of the beam ($v_i'(z)$),

$$v'_i(z) = \left(\frac{\mu\varepsilon_i + \mu\varepsilon_{i-1}}{2R \cdot 10^6}\right)\Delta z_i + v'_{i-1}(z) \tag{3}$$

where:

The factor $\frac{1}{10^6}$ is the conversion factor from με to ε;

$R = 0.041\,m$ is the radius of the tube-sensor system, given by the sum of the radius of the aluminum tube $R_1 = 0.04\,m$ and an estimate of half the sensor radius set equal to $R_2 = 0.001\,m$.

$$\Delta z_i = z_i - z_{i-1} \tag{4}$$

Moreover, by a second numerical integration, one obtains the displacement function:

$$v_i(z) = \left(\frac{v'_i(z) + v'_{i-1}(z)}{2}\right)\Delta z_i + v_{i-1}(z) \tag{5}$$

The integration requires the knowledge of the initial value of displacement and its derivative that must be evaluated by imposing the following boundary condition:

$$\begin{cases} v(0) = 0 \\ v(l) = 0 \end{cases} \tag{6}$$

2.3 Second Test: Horizontal inclinometer equipped with GG transducer

The tested specimen consisted of an inclinometer casing tube equipped with standard displacement transducers. The tube (with the same cross-section of the previous experiment) has consisted of three segments joined to form the whole cylinder. The three segments have been fastened, employing two collars that formed a little disturbance to the alignment of the transducer.

Preprints (www.preprints.org) | NOT PEER-REVIEWED | Posted: 4 June 2020

Peer-reviewed version available at Appl. Sci. 2020, 10, 4498; doi:10.3390/app10134498

The optical fiber-based transducers instrumented the inclinometer casing. The transducer was fastened to the cylinder along its generatrix. Table 3 below reported the geometry data of the structure used for the test:

Tab. 3 Second test – geometrical parameters

Length [mm]	Radius [mm]	Thickness [mm]	Inertia [cm⁴]
7500	80	3	56.4871

Tab. 4: second test – transducer parameters

Type	Structural glue	Fiber	Length [mm]	Optical fiber	Resin	Control unit	Resolution [mm]
GG	ADEKIT 140 by Axon (bi-component epoxy resin)	Glass – Glass (mat220 fiberglass polyester composite)	6500	G.652 single-mode optical fibers	BIRESIN® CR80 (AXSON)	OPTO SENSING	50

The GG transducer is made accordingly to the scheme reported in figure 6. The inclinometer measures, in terms of displacements, have been converted into strains by numerical derivation; then, they were compared with the transducer output. The inclinometer, indeed, furnishes displacement measures that must be elaborated to convert into strain by means of derivation with respect to the length coordinate.

The experiment consisted of the application of a constrained displacement at the first end of the structure while the opposite end was kept clamped; namely, no displacement neither rotations are allowed. The applied displacement runs from 0 to 0.014?*m*

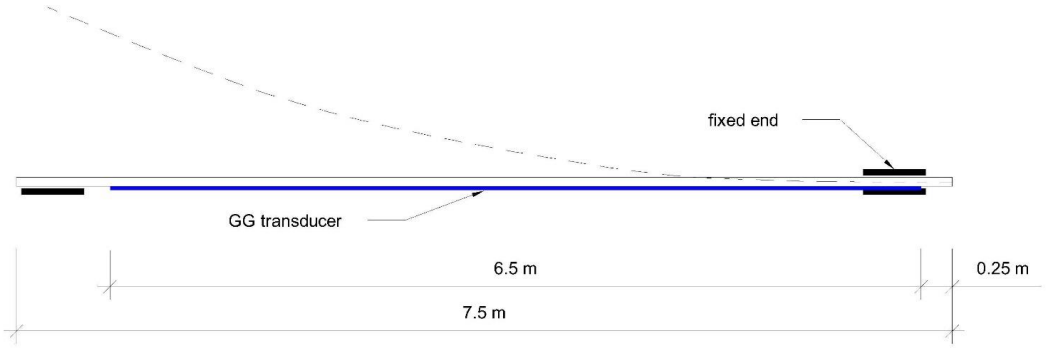

Fig. 6 Second test - Structural scheme

2.4 Third Test: Vertical Inclinometer equipped with GG and CG transducer

One of the most critical aspects regarding the evaluation of the experimental results is structural identification. That means to determine a numerical model suitable for providing accurate predictions on the behavior of the structural element subjected to specific stresses. The identification of the structural model consists of applying inverse calculation techniques to correlate the test results to the actual stresses or displacements. This approach consists of the identification of mechanical properties, to modify their values appropriately, to minimize a suitable functional norm of the difference between the experimental results and the expected theoretical ones. Therefore,

Preprints (www.preprints.org) | NOT PEER-REVIEWED | Posted: 4 June 2020

Peer-reviewed version available at Appl. Sci. 2020, 10, 4498; doi:10.3390/app10134498

based on experimental data and reliable information on geometry and materials, it is possible to define a predictive model that represents the behavior of the tested elements.

The third experiment has been designed to apply structural identification techniques to the measured data. To the scope, the inclinometer has been disposed vertically and fixed to support using flexible collars, the structure was subjected to prescribed displacements at some of the supports whilst the remainder was kept fixed. The inclinometer pipe has been instrumented with the proposed transducer and with its traditional displacement acquisition system.

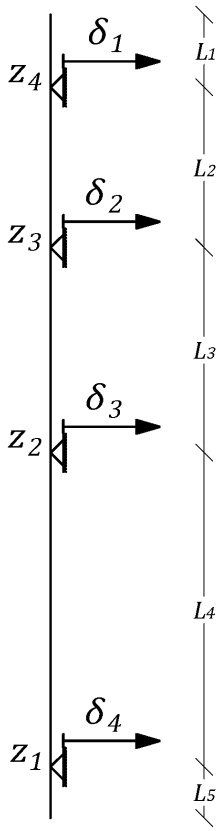

Fig. 7 third test – structural identification

Figure (7) represents the structural model of the third experiment. Prescribed displacements acted on the structure. In particular, the displacements δ_1 and δ_2 are the prescribed displacements of $2.5\,cm$ that have been applied to the pipe. The displacements δ_3 δ_4 are unknown, since the flexibility of the supporting devices. The displacement depended on the fastening devices that evidenced rewardable mobility. The structural identification consisted of finding the minimal difference norm between measured and calculated strain along the beam. As design variables, we chose, besides the constraint displacements $\delta_i, i \in \{ ,\ldots, \}$, the span measures L_1, L_2, L_3, L_4, L_5 (Figure 7).

The tested specimen was equipped with two kinds of transducers as shown in table 6

Tab. 5 third test – geometrical parameters

Length [mm]	Radius [mm]	Thickness [mm]	Inertia [cm⁴]
7600	80	3	56.4871

Preprints (www.preprints.org) | NOT PEER-REVIEWED | Posted: 4 June 2020

Peer-reviewed version available at Appl. Sci. 2020, 10, 4498; doi:10.3390/app10134498

The test set up is represented in figure 8, where the inclinometer cylinder has been schematically represented as a one-dimensional beam subjected to prescribed boundary displacements.

Like in the previous example, the procedure consists of comparing the strain obtained from displacement measurements via space derivation, to the strain measured with the NSHT.

The measured strain using the CG and the GG transducers has been acquired accordingly to two different setups. The first setup concerned CG transducer that has been fastened to the cylinder starting at a depth of 250 mm, see figure 8a). The second set up is described in fig. 8b).

Tab. 6 third test – specimen parameters

Type	Structural glue	Fiber	Length [mm]	Optical fiber	Resin	Control unit	Resolution [mm]
GG	ADEKIT 140 by Axon	Glass – Glass (mat220 fiberglass polyester)	4000	G.652 single-mode optical fibers	BIRESIN® CR80 (AXSON)	OPTO SENSING OSD-1"	400
CG	ADEKIT 140 by Axon	Carbon – Glass (biaxial 200 carbon fiber composite and two mat100 fiberglass polyester composite)	5250	G.657 single-mode optical fibers	BIRESIN® CR80 (AXSON)	OPTO SENSING OSD-1"	400

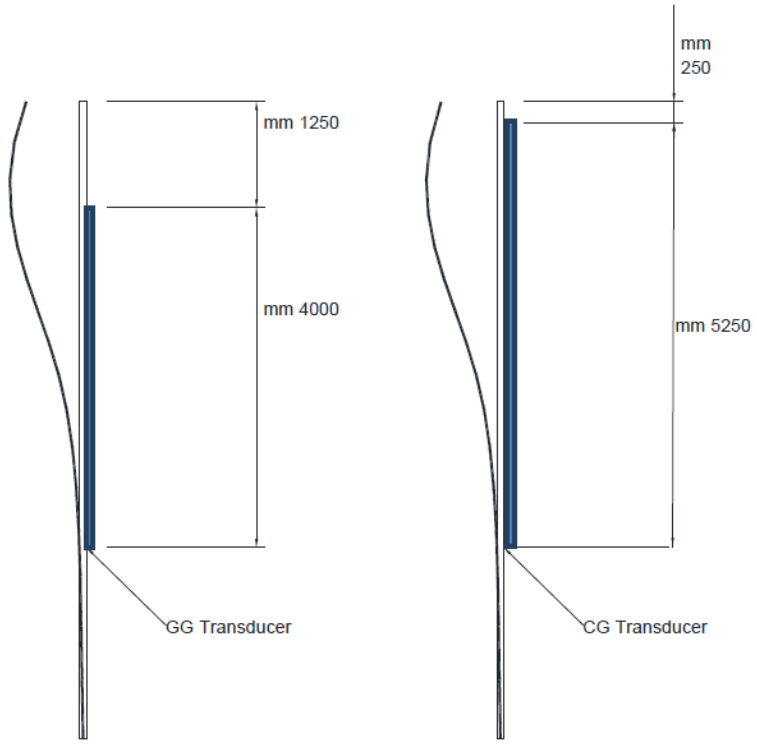

Fig. 8: structural schemes of vertical inclinometer

Preprints (www.preprints.org) | NOT PEER-REVIEWED | Posted: 4 June 2020

Peer-reviewed version available at Appl. Sci. 2020, 10, 4498; doi:10.3390/app10134498

3. Results and discussion

The results of measurements and calculations obtained from the tests have been reported in diagrams in order to make a better comparison both in quantitative and qualitative terms.

3.1. Test 1: Beam deflection and imposed deformation

As described in the previous section, the experiment concerned a three supports beam subjected to the central support settlement. The curved line of the beam centroids was calculated by the beam theory, and it was obtained from the experimental results through numerical integration of the curvature calculated from the measured strain. In the pictures below (figures 9, 10, and 11), the data comparison related to the 2.5, 4.5, and 6.5 cm displacements is shown.

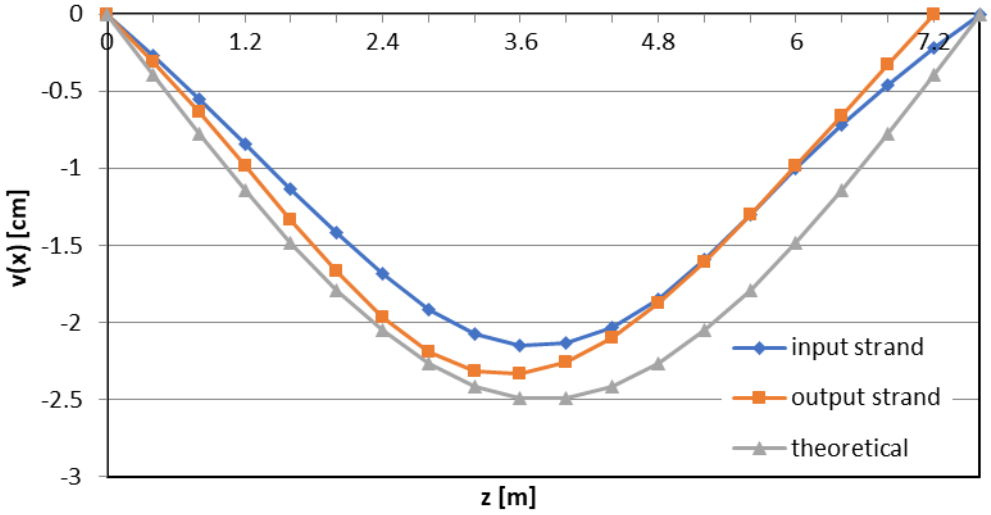

Fig. 9 Centerline deformation imposed at 2.5 cm

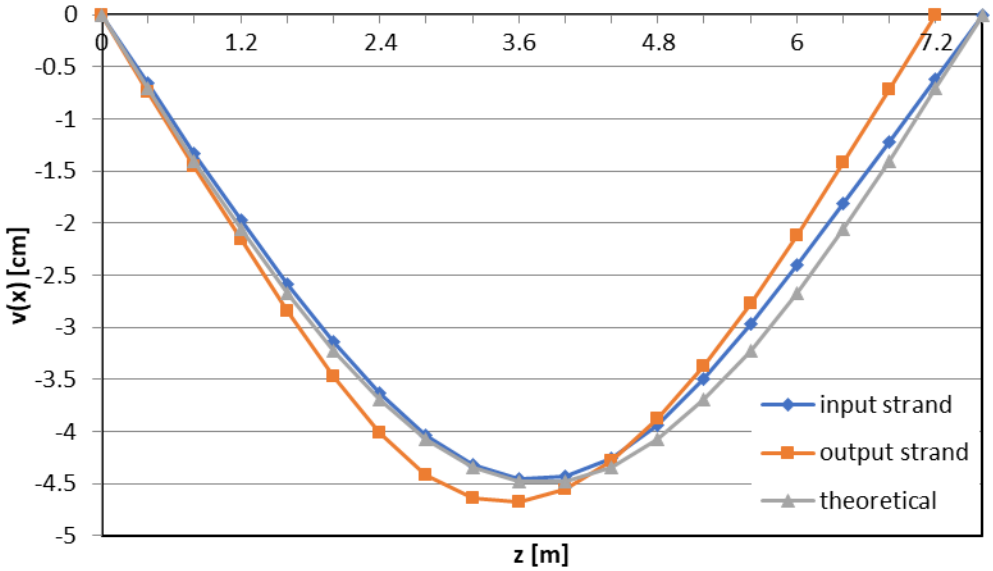

Fig. 10 Centerline deformation imposed at 4.5 cm

Preprints (www.preprints.org) | NOT PEER-REVIEWED | Posted: 4 June 2020

Peer-reviewed version available at Appl. Sci. 2020, 10, 4498; doi:10.3390/app10134498

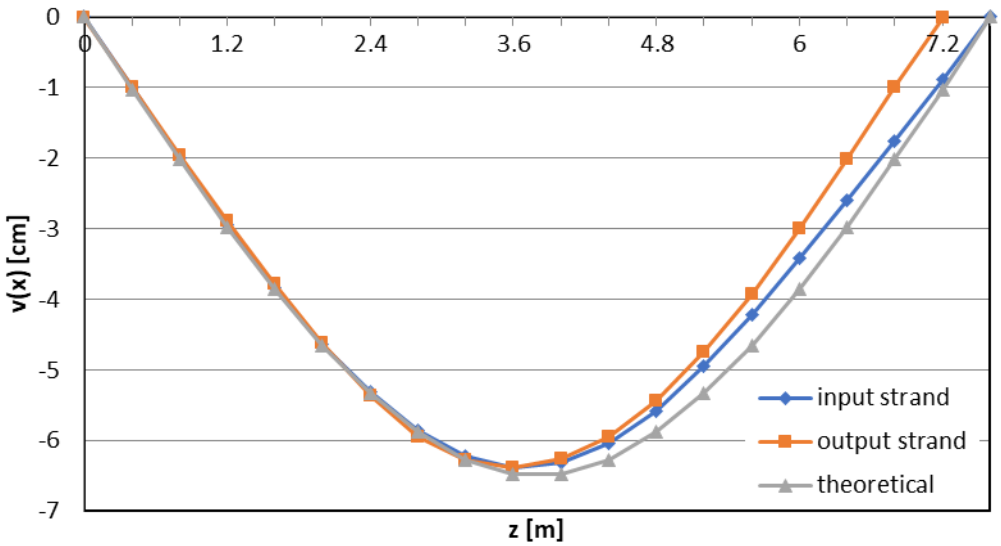

Fig. 11 Centerline deformation imposed at 6.5 cm

The difference shown in the graph between the measured values and the theoretical model could undoubtedly be attributed to the fact that the theoretical values refer to the axis of the pipe, while the measured ones refer to the fiber positioned at the boundary of the cross-section.

3.2. *Test 2: Horizontal Inclinometer measurement and GG transducer*

In figure 12, the GG transducer strain measures from NSHT have been compared with the strain calculated from the displacement derivative of the inclinometer measurements.

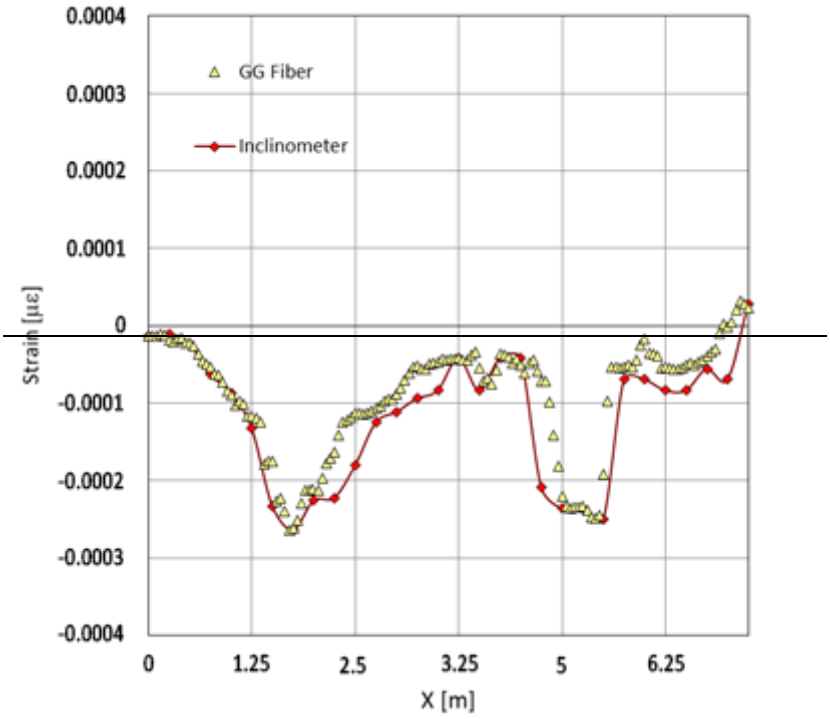

Fig. 12 Strain diagram GG transducer

The diagram shows the agreement of the strain measurements from the GG transducer and the calculated strain from the inclinometer measurements. The percentage differences between the two

Preprints (www.preprints.org) | NOT PEER-REVIEWED | Posted: 4 June 2020

Peer-reviewed version available at Appl. Sci. 2020, 10, 4498; doi:10.3390/app10134498

sets showed picks of 20% in correspondence of metallic collars that fastened the inclinometer pipe. If we considered only smooth points, the average difference percentage attained 1%.

3.2. *Test 3: Vertical Inclinometer measurement and GG and CG transducers*

In the following figure 8 and figure 9, show the comparison of the strain measures obtained using CG and GG transducers with the strain arising from the derivative of the displacement obtained by the inclinometer cylinder. In the figures below, the transducer measures refer to two pickup phases, namely fiber 1 and fiber 2; subsequently, the two measures have been averaged, resulting in the fiber average data set. Furthermore, in the diagram, the strain obtained by the inclinometer displacement measure has been drawn as well.

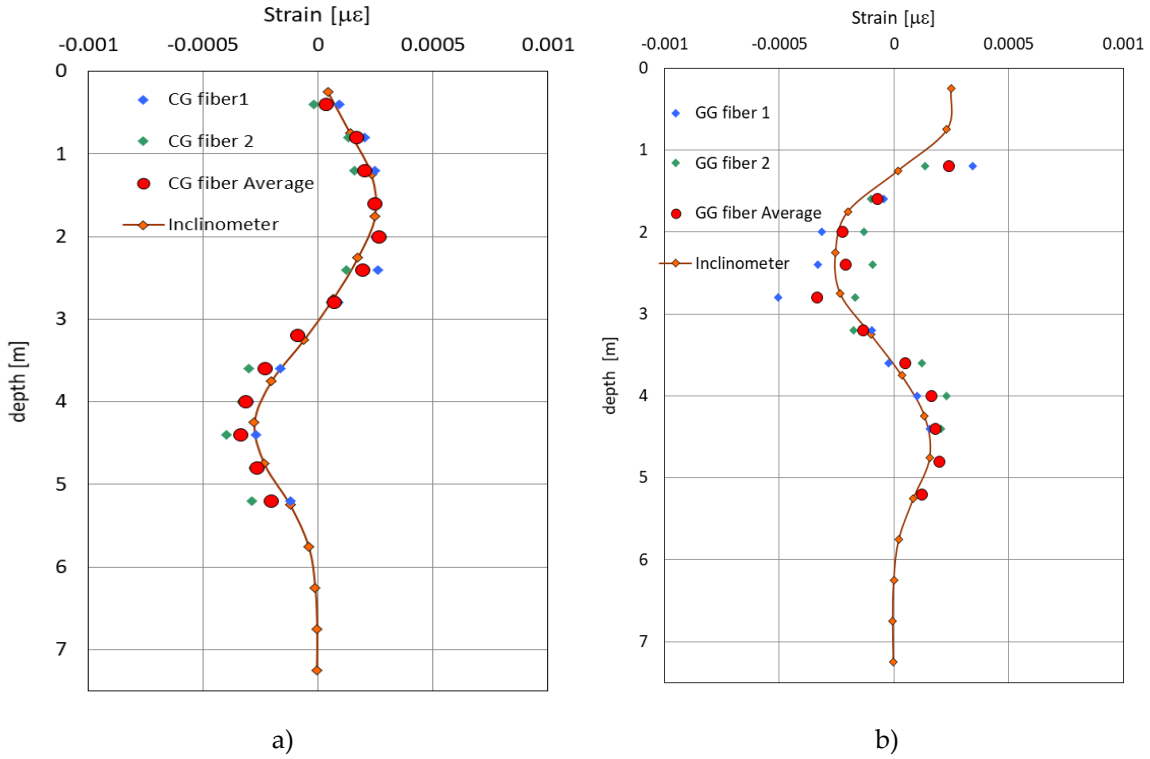

a) b)

Fig. 13 Experiment 3 strain diagram: a) CG transducer, b) GG transducer

From the comparison of Figures 8a and 8b, it resulted that the strain obtained using the CG transducer presents fewer errors due to the quality of the used fiber and to the transducer building technique than using the GG transducer. The GG transducer, indeed, has been realized with G.652 fiber that suffers a more significant loss of signal in the presence of relatively high curvatures. The CG transducer has been made of G.657 fiber that presents less loss of signal in the presence of curvatures of the fiber. Moreover, the manufacturing process in the case of GG transducer has suffered that some little but not negligible localized curvatures of the fiber occurred. Henceforth, the diagrams allow recognizing that the CG transducer, equipped with ITU G.657 fiber, furnishes a better strain map than the GG transducer equipped with G.652 fiber. The worst result, at the GG transducer, is obtained at a position near to the collar joining the cylinder segments, at a point about 1250?*mm* from the inclinometer casing top.

5. Conclusions

The present paper showed the feasibility of using fiber optical sensors in structural behavior evaluation and monitoring; the purpose of NSHT application is to have continuous in time and space measurements of structural stress. Indeed, the transducer allows monitoring the strain and,

Preprints (www.preprints.org) | NOT PEER-REVIEWED | Posted: 4 June 2020

Peer-reviewed version available at Appl. Sci. 2020, 10, 4498; doi:10.3390/app10134498

consequently, the stress directly. One does not have the necessity of correlating measured displacement to the actual safety of the structures like it is often done with conventional in the field test campaign involving displacement transducers.

However, one can reverse the perspective considering that the information obtained was an instrument for the structural condition evaluation commuting, strain into displacement in every section using indirect calculation, such as the numerical derivation of the data.

The fitting between theoretical and experimental results showed that the strain measurements are reliable for displacement calculation. The measured strain revealed to have low error and uncertainty thanks to NSHT. Finally, the proposed sensor allowed the user to read displacements and all related structural information along the axis of the structure instead of the section strain

Author Contributions: For research articles with several authors, a short paragraph specifying their individual contributions must be provided. The following statements should be used "Conceptualization, V.M., L.O., and E.D.; methodology, V.M., L.O., and E.D.; software, V.M., L.O., E.D., P.F., R.Z., L.D., M.D. ,M.M. and , and E.C.; validation, V.M., A.C., L.O., E.D., P.F., R.Z., L.D., M.D., and E.C.; formal analysis, V.M., L.O., E.D., P.F., R.Z., L.D., M.D., and E.C.; investigation, V.M., L.O., E.D., P.F., R.Z., L.D., M.D., and E.C.; resources, V.M., L.O., E.D., P.F., R.Z., L.D., M.D., and E.C.; data curation, V.M., L.O., E.D., P.F., R.Z., L.D., M.D., and E.C.; writing—original draft preparation, V.M., L.O., E.D., P.F., R.Z., L.D., M.D., and E.C.; writing—review and editing, V.M., L.O., E.D., P.F., R.Z., L.D., M.D., and E.C.; visualization, V.M., L.O., E.D., P.F., R.Z., L.D., M.D., and E.C.; supervision, V.M., L.O., and E.D.; project administration, V.M., L.O., and E.D.; funding acquisition, V.M., L.O., and E.D. All authors have read and agreed to the published version of the manuscript

Funding: This research was funded by the Università degli Studi della Campania "L.Vanvitelli", grant Programma VALERE: "VAnviteLli pEr la RicErca", DDG n. 516 – 24/05/2018.

Conflicts of Interest: The authors declare no conflict of interest.

References

1. Olivares L.; Damiano E.; Netti N.; de Cristofaro M. Geothecnical Properties of two pyroclastic deposits involved in catastrophic flowslides for implementation in early warning systems *Geosciences* **2019**, 9-24, doi:10.3390

2. Liu B.; Xi P.; Guo Y.; Zhang D.; Field test study of soil displacement screw pile using distributed optical fiber based on BOTDA technique *Journal of Central South University* **2017**, *48*, 779-786, doi:10.11817

3. Damiano E.; Avolio B.; Minardo A.; Olivares L.; Picarelli L.; Zeni, L. A Laboratory Study on the Use of Optical Fibers for Early Detection of Pre-Failure Slope Movements in Shallow Granular Soil Deposits. *Geotechnical Testing Journal* **2017**, *40*, doi:10.1520/GTJ20160107

4. Damiano E.; Greco R.; Guida A.; Olivares L.; Picarelli L. Investigation on rainwater infiltration into layered shallow covers in pyroclastic soils and its effect on slope stability *Engineering Geology*, **2017** ,220, p. 208-218, doi: 10.1016/j.enggeo.2017.02.006

5. Damiano E.; Mercogliano P.; Netti N. Olivares L.; A "simulation chain" to define a Multidisciplinary Decision Support System for landslide risk management in pyroclastic soils *Natural Hazards and Earth System Sciences*, 12-4, 989-1008,

6. Olivares L.; Damiano E.; Mercogliano P.; Picarelli L.; Netti N.; Schiano P.; Savastano V.; Cotroneo F.; Manzi M. P. A simulation chain for early prediction of rainfall-induced landslides *Landslides*, **2014,**11-5, 765-777

7. Minutolo V.; Di Ronza S.; Eramo C.; Ferla P.; Palladino S.; Zona R. The use of destructive and non-destructive testing in concrete strength assessment for a school building *International Journal of Advanced Research in Engineering and Technology*, **2019**,*10*-6,252-267

Preprints (www.preprints.org) | NOT PEER-REVIEWED | Posted: 4 June 2020

Peer-reviewed version available at Appl. Sci. 2020, 10, 4498; doi:10.3390/app10134498

8. Smarsly K.; Lehner K.;Hartmann D. Structural Health Monitoring based on Artificial Intelligence Techniques *Computing in Civil Engineering* ,**2007**,

9. Allen R. M. The Potential for Earthquake Early Warning in Southern California *Science*, **2003**, 300, pp. 786-789,

10. Bernini R.; Minardo A. ; Zeni L.; Metodo di ricostruzione del profilo di shift Brillouin in fibra ottica a partire da misure di scattering di Brillouin eseguite nel dominio della frequenza patent N. 0001408170. **2014.**

11. Optosensing; Apparato per la misura di profilo di shift brillouin in fibra ottica basato sull'acquisizione in tempo reale del segnale differenziale. Patent N. 0001422139. **2016**.

12. Iten M. Puzrin A. M. BOTDA road-embedded strain sensing system for landslide boundary localization **2009.**

13. Farhadiroushan M.; Johansson S. Seepage and strain monitoring in embankment dams using distributed sensing in optical fibers-theoretical background and experiences from some installations in Sweden *International Symposium on Dam Safety and Detection of Hidden Troubles*, **2005**, Xi'an, China

14. Gao P.; The Application of Distributed Optical Fiber Sensing in Seepage Flow Monitoring System *International Journal of Digital Content Technology and its Applications*, **2012** ,*6-12*,75-181,.

15. Lee K. M.; Manjunath V. R. Experimental and numerical studies of geosynthetic-reinforced sand slopes loaded with a footing *Canadian Geotechnical Journal*, **2000**, *37-4*,828-842,

16. Moser F.; Lienhart W.; Woschitz H.; Schuller H. Long-term monitoring of reinforced earth structures using distributed fiber optic sensing, *Journal of Civil Structural Health Monitoring*, **2016**, *6-3*, 321-327

17. Pei H.; Cui P.; Yin J.; Zhu H.; Chen X.; Pei L.; Xu D. Monitoring and warning of landslides and debris flows using an optical fiber sensor technology *Journal of Mountain Science*, **2011** *8-5*, 728- 738

18. Zeni L.; Picarelli L.; Avolio B.; Coscetta A.; Papa R.;Zeni G.; Di MaioC.; Vassallo R.;Minardo A. Brillouin optical time-domain analysis for geotechnical monitoring *Journal of Rock Mechanics and Geotechnical Engineering*, **2015**, *7-4*, 458-462

19. Shi B.; Sui H.; Liu J.; Zhang D. The BOTDR-based distributed monitoring system for slope engineering *in IAEG* **2006**, Nottingham, UK,

20. Pei H.; Yin J.; Zhu H.; Hong C. Development and Application of an Optical Fiber Sensor Based In- Place Inclinometer for Geotechnical Monitoring *in Geo-Frontiers* **2011**, Reston, VA

21. Bao H.; Dong X.; Shao L.-Y.; Zhao C.-L., Chan C. C.; Shum P., Temperature-Insensitive 2-D Pendulum Clinometer Using Two Fiber Bragg Gratings *IEEE Photonics Technology Letters*, **2010**, *22-12*, 863-865

22. Di Ronza S.; Eramo C.; Minutolo V.; Palladino S.; Totaro E., Ferla P.; Zona R.; Ronga T.; Pomicino C.C. Experimental tests on gully tops and manhole TOPS devices according to EN124 standard *International Journal of Advanced Research in Engineering and Technology*, **2020**, *11-2*, 276-295

23. Guo C.; Chen D.; Shen C.; Lu Y.; Liu H., Optical inclinometer based on a tilted fiber Bragg grating with a fused taper *Optical Fiber Technology*, **2015**, *24*, 30-33

24. Damiano E.; Avolio B.; Minardo A.; Olivares L.; Picarelli L.; Zeni L., A Laboratory Study on the Use of Optical Fibers for Early Detection of Pre-Failure Slope Movements in Shallow Granular Soil Deposits *Geotechnical Testing Journal*, **2017**, *40-4*, 20160107

Preprints (www.preprints.org) | NOT PEER-REVIEWED | Posted: 4 June 2020

Peer-reviewed version available at Appl. Sci. 2020, 10, 4498; doi:10.3390/app10134498

25. Schenato L.; Palmieri L.; Camporese M.; Bersan S.; Cola S.; Pasuto A.; Galtarossa A.; Salandin P.; Simonini P.; Distributed optical fiber sensing for early detection of shallow landslides triggering *Scientific Reports*, **2017**, *7-1*, 14686

26. Zhu H.-H.; Shi B.; Zhang J.; Yan J.-F.; Zhang C.-C. Distributed fiber optic monitoring and stability analysis of a model slope under surcharge loading *Journal of Mountain Science*, **2014**, *11-4*, 979- 989

27. Katunin A.; Dragan K.; Dziendzikowski M. Damage identification in aircraft composite structures: A case study using various non-destructive testing techniques *Composite Structures*, **2015**, *127*, 1-9

28. Polimeno U.; Meo M. Detecting barely visible impact damage detection on aircraft composites structures *Composite Structures*,**2009**, 91-4,398-402

29. Avdelidis N.; Almond D.; Dobbinson A.; Hawtin B.; Ibarra-Castanedo C.; Maldague X. Aircraft composites assessment by means of transient thermal NDT *Progress in Aerospace Sciences*, **2004,** 40-3, 143-162

30. Usamentiaga R.; Venegas P.; Guerediaga J.; Vega L. ; López I., Automatic detection of impact damage in carbon fiber composites using active thermography *Infrared Physics and Technology*, **2013,** 58, 36-46

31. Trendafilova I., Cartmell M.; Ostachowicz W. Vibration-based damage detection in an aircraft wing scaled model using principal component analysis and pattern recognition *Journal of Sound and Vibration*, **2008**, 313, 3-5, 560-566

32. Loutas T., Panopoulou A., Roulias D. ; Kostopoulos V. Intelligent health monitoring of aerospace composite structures based on dynamic strain measurements *Expert Systems with Applications*, **2012**, 39-9, 8412-8422

33. Ratcliffe C.; Heider D.; Crane R.; Krauthauser C.; Yoon M. K. ; Gillespie J. W. Investigation into the use of low cost MEMS accelerometers for vibration based damage detection *Composite Structures*, **2008**.

34. Zou Y., Tong L.; Steven G. Vibration-based model-dependent damage (delamination) identification and health monitoring for composite structures - a review *Journal of Sound and Vibration*,**2000**,*230-2*, 357-378

35. Westbrook P. S.; Kremp T.; Feder K. S.; Ko W.; Monberg E. M.; Wu H.; Simoff D. A.; Taunay T. F. ; Ortiz R. M. Continuous Multicore Optical Fiber Grating Arrays for Distributed Sensing Applications *Journal of Lightwave Technology*, **2017**, *35-6*, 1248-1252

36. Floris I.; Sales S.; Calderón P. A. ; Adam J. M. Measurement uncertainty of multicore optical fiber sensors used to sense curvature and bending direction *Measurement*, **2019** ,*132*, 35-46,

37. Hong C.-Y., Yin J.-H.; Zhang Y.-F.Deformation monitoring of long GFRP bar soil nails using distributed optical fiber sensing technology *Smart Materials and Structures*, **2016** , *25- 8*, 085044.

38. Huang X.; Yang M.; Feng L.; Gu H.; Su H.; Cui X.; Cao W. Crack detection study for hydraulic concrete using PPP-BOTDA *Smart Structures and Systems*, **2017**, *20- 1*, 75-83

39. Fajkus M.; Nedoma J.; Mec P.; Hrubesova E.; Martinek R.; Vasinek V. Analysis of the highway tunnels monitoring using an optical fiber implemented into primary lining *Journal of Electrical Engineering*, **2017,** *68-5*, 364-370

40. Stern Y., London Y.; Preter E.; Antman Y.; Diamandi H.; Silbiger M.; Adler G.; Levenberg E.; Shalev D.; Zadok A. Brillouin Optical Correlation Domain Analysis in Composite Material Beams *Sensors*,**2017** ,*17-10*, 2266.

Preprints (www.preprints.org) | NOT PEER-REVIEWED | Posted: 4 June 2020

Peer-reviewed version available at *Appl. Sci.* **2020**, *10*, 4498; doi:10.3390/app10134498

41. Dragic P. ; Ballato J. A Brief Review of Specialty Optical Fibers for Brillouin-Scattering-Based Distributed Sensors *Applied Sciences*, **2018**, *8-10*, 1996

42. Barrias A., Casas J. Villalba S. A Review of Distributed Optical Fiber Sensors for Civil Engineering Applications *Sensors*, **2016**, *16- 5*, 748

43. Bao X.; Chen L. Recent progress in optical fiber sensors based on Brillouin scattering at University of Ottawa *Photonic Sensors*, **2011**, *1-2*, 102-117

44. Banerji P.; Chikermane S.; Grattan K.; Tong S.; Surre F.; Scott R. Application of fiber-optic strain sensors for monitoring of a pre-stressed concrete box girder bridge *in 2011 IEEE SENSORS Proceedings*, **2011**.

45. Coscetta A.; Minardo A.; Olivares L.; Mirabile M.; Longo M.; Damiano M.; Zeni L. Wind Turbine Blade Monitoring with Brillouin-Based Fiber-Optic Sensors *Journal of Sensors*, **2017**, 1-5

46. Bremer K.; Weigand F.; Zheng Y.; Alwis L.; Helbig R.; B. Roth Structural Health Monitoring Using Textile Reinforcement Structures with Integrated Optical Fiber Sensors *Sensors*, **2017**, *17-2*, 345

47. Rodríguez G.; Casas J. R.; Villaba S.; Cracking assessment in concrete structures by distributed optical fiber *Smart Materials and Structures*, **2015**, *24-3*, 035005

48. Wang Y.; Jin B.; Wang Y.; Wang D.; Liu X.; Dong Q. Distributed fiber-optic vibration detection system *in 2016 13th International Conference on Ubiquitous Robots and Ambient Intelligence (URAI)*, **2016**.

49. Ruocco E.; Minutolo V. Buckling Analysis of Mindlin Plates Under the Green–Lagrange Strain Hypothesis *International Journal of Structural Stability and Dynamics*, **2015**, *15-06*, 1450079

50. Uva G.; Porco F.; Fiore A.; Porco G., Structural monitoring using fiber optic sensors of a pre-stressed concrete viaduct during construction phases *Case Studies in Nondestructive Testing and Evaluation*, **2014**, *2*, 27-37

51. Glišić B., Hubbell D., Sigurdardottir D. H.; Yao Y. Damage detection and characterization using long-gauge and distributed fiber optic sensors *Optical Engineering*, **2013**, *52-8*, 087101

52. Coscetta A.; Damiano E.; De Cristofaro M.; Di Gennaro L.; Esposito L.; Ferla P.; Giarusso G.A.; Iavazzo L.; Minutolo V.; Mirabile M.; Olivares L.; Zona R. An Integrated structural and geotechnical early-warning system for deep-seated landslides **2020** *under submission*

53. Minutolo V.; Ruocco; E.; Zeni; L.; Strain measure in laboratory experiments on concrete beams by means of optical fiber sensors *AIMETA 2017 - Proceedings of the 23rd Conference of the Italian Association of Theoretical and Applied Mechanics* **2017**, *4*, 472-479

54. Bernini, R.; Minardo, A.; Ciaramella, S.; Minutolo, V.; Zeni, L. Distributed strain measurement along a concrete beam via stimulated brillouin scattering in optical fibers, *International Journal of Geophysics*, **2011**, doi:10.1155/2011/710941

55. Bernini, R.; Fraldi, M.; Minardo, A.; Minutolo, V.; Nunziante, L.; Zeni, L., Identification of defects and strain error estimation for bending steel beams using time-domain Brillouin distributed optical fiber sensors, *Smart Materials and Structures*, **2006** , *15 -2*, 612-622

56. Bernini R.; Fraldi M.; Minardo A.; Minutolo V.; Nunziante, L.; Zeni, L. Damage detection in bending beams through Brillouin distributed optic-fiber sensor, Bridge Structures, **2005** ,*1-3*,355-363